



Indian Institute Of Technology, Ropar

Department of Physics

CP301

Study of Growth Techniques and Structural  
Analysis of 2D van der Waals Materials

Palavalasa Bhargav Naidu

*Supervisor:* DR. Ritu Gupta

This report is submitted in partial fulfilment of the requirements for the coursework  
CP301 - "Development Engineering product" as part of the  
Engineering Physics program at *Indian Institute Of Technology, Ropar*

May 13, 2025

## **Declaration**

I, Palvalasa Bhargav Naidu , of the Department of Physics, Indian Institute Of Technology Ropar, confirm that this is my own work and figures, tables, equations, code snippets, artworks, and illustrations in this report are original and have not been taken from any other person's work, except where the works of others have been explicitly acknowledged, quoted, and referenced. I understand that if failing to do so will be considered a case of plagiarism. Plagiarism is a form of academic misconduct and will be penalised accordingly.

I give consent to a copy of my report being shared with future students as an exemplar.

I give consent for my work to be made available more widely to members of IIT RPR and public with interest in teaching, learning and research.

Palavalasa Bhargav Naidu  
May 13, 2025

## Abstract

Two-dimensional (2D) van der Waals (vdW) materials represent a rapidly expanding class of layered compounds with exceptional properties distinct from their bulk counterparts. These materials exhibit strong in-plane bonding and weak out-of-plane interactions, enabling tunable physical behaviors and applications in areas such as spintronics, quantum computing, and superconductivity. This project focuses on the crystallographic analysis of PbTaSe<sub>2</sub>, a layered 2D vdW material, using powder X-ray diffraction (XRD) and FullProf refinement techniques. Due to the lack of access to experimental growth infrastructure, the project was conducted through a combination of literature review on growth techniques and analysis of pre-synthesized experimental samples. Initial training and method validation were done using Vanadium as a standard reference sample. For PbTaSe<sub>2</sub>, phase identification was carried out using Match! software and refinement was performed using the FullProf suite. Significant challenges emerged from preferred orientation (texture) along the *I*-direction, impurity peaks due to oil contamination, and ghost peaks caused by beta filter inefficiency. These were addressed using the March–Dollase correction model, impurity filtering with Origin software, and exclusion of peak regions violating Bragg's law. The refined lattice parameters were found to be  $a = 3.44 \text{ \AA}$  and  $c = 9.40 \text{ \AA}$ , in close agreement with standard values. This study highlights the effectiveness of computational refinement methods in extracting accurate structural information in the absence of direct synthesis and demonstrates the need for careful data treatment when working with anisotropic 2D materials.

**Keywords:** 2D materials, van der Waals compounds, X-ray diffraction, Rietveld refinement, crystallographic texture

**Report's total word count: 11,452 words**

**GitLab Repository:** <https://github.com/Bhargav-Naidu-29/Growth-Techniques-and-Structural-Ana>

## **Acknowledgements**

I would like to express my sincere gratitude to Dr. Ritu Gupta, my project supervisor, for her continuous guidance, valuable insights, and constant support throughout the course of this project. Her expertise in the field of materials science and encouragement at every stage were instrumental in shaping the direction of my work.

I am also deeply thankful to Mrs. Reena, for her patience, technical assistance, and helpful discussions, especially during the FullProf refinement and XRD data analysis.

I extend my appreciation to the Department of Physics at the Indian Institute of Technology Ropar for providing me with the academic environment and infrastructure that enabled me to pursue this project.

# Contents

<b>List of Figures</b>	<b>vi</b>
<b>List of Tables</b>	<b>vii</b>
<b>1 Introduction</b>	<b>1</b>
1.1 Background . . . . .	1
1.2 Problem Statement . . . . .	1
1.3 Aims and Objectives . . . . .	1
1.4 Solution Approach . . . . .	2
1.5 Summary of Contributions and Achievements . . . . .	2
1.6 Organization of the Report . . . . .	2
<b>2 Literature Review</b>	<b>3</b>
2.1 State-of-the-art Synthesis Techniques for van der Waals Materials . . . . .	3
2.1.1 Chemical Vapor Transport (CVT) . . . . .	3
2.1.2 Flux Growth Method . . . . .	3
2.1.3 Chemical Vapor Deposition (CVD) . . . . .	3
2.1.4 Other Methods . . . . .	4
2.2 Crystallographic Texture and Its Impact on XRD Analysis . . . . .	4
2.3 Context and Relevance to the Present Work . . . . .	4
2.4 Critique of Existing Work . . . . .	5
2.5 Significance for This Project . . . . .	5
<b>3 Methodology</b>	<b>6</b>
3.1 Synthesis of PbTaSe <sub>2</sub> Single Crystals . . . . .	6
3.2 X-Ray Diffraction (XRD) . . . . .	6
3.3 Phase Identification . . . . .	7
3.4 Structure Refinement using FullProf . . . . .	8
3.5 Conclusion of Methodology . . . . .	8
<b>4 Results</b>	<b>9</b>
4.0.1 XRD Patterns of Vanadium and PbTaSe <sub>2</sub> . . . . .	9
4.0.2 Phase Identification Using Match! Software . . . . .	11
4.0.3 Comparison of Experimental and Reference Data . . . . .	12
4.0.4 Refined XRD Output Summary . . . . .	12
<b>5 Discussion and Analysis</b>	<b>13</b>
5.1 Comparison with Reference Pattern . . . . .	13
5.2 Texture and Preferred Orientation in Layered Materials . . . . .	14
5.3 Correction of Texture using FullProf . . . . .	14

5.4 Contamination by Oil and Peak Removal using Origin . . . . .	14
5.5 Beta Filter Inefficiency and Bragg's Law Justification . . . . .	15
5.6 Effect on Structural Refinement . . . . .	15
5.7 Summary . . . . .	16
<b>6 Conclusion</b>	<b>17</b>
<b>References</b>	<b>18</b>

# List of Figures

2.1	Graphical representation of preferred orientation for nanoparticles having different shapes: (a) spheres, (b) cubes, and (c) rods. Simulated X-ray diffraction patterns for varying degrees of alignment (i.e., preferred orientation) of wurtzite CdS particles along specific crystallographic directions: (d) [100], (e) [001], and (f) [110]. Source: Li et al. (2020)	4
3.1	Diagram of XRD Instrumentation Components. Source" Perkins et al. (2019)	7
4.1	Raw XRD pattern of Vanadium sample . . . . .	9
4.2	Refined XRD pattern for Vanadium sample with $\chi^2 = 1.28$ . . . . .	10
4.3	Raw XRD pattern of PbTaSe <sub>2</sub> sample (with impurity peaks) . . . . .	10
4.4	Refined XRD pattern for PbTaSe <sub>2</sub> sample with $\chi^2 = 18.3$ . . . . .	10
4.5	Phase identification of Vanadium using Match! software . . . . .	11
4.6	Phase identification of PbTaSe <sub>2</sub> using Match! software . . . . .	11
5.1	Left: Refined experimental XRD pattern of PbTaSe <sub>2</sub> ; Right: Simulated pattern from Materials Project . . . . .	13
5.2	Peak removal process using Origin . . . . .	14
5.3	Effect of beta filter inefficiency: ghost peaks and shoulders in raw PbTaSe <sub>2</sub> data	15

# List of Tables

4.1 Comparison of Experimental and Reference Parameters for PbTaSe <sub>2</sub> . . . . .	12
4.2 Comparison of Experimental and Reference Parameters for Vanadium . . . . .	12

# Chapter 1

## Introduction

### 1.1 Background

Two-dimensional (2D) materials, especially those belonging to the van der Waals (vdW) family, have revolutionized condensed matter physics and materials science due to their exotic electronic, optical, and magnetic properties. These materials exhibit weak interlayer bonding, allowing exfoliation into atomically thin sheets, making them attractive for next-generation applications in transistors, quantum computing, and spintronics.

Among these, PbTaSe<sub>2</sub> has gained recent attention due to its non-centrosymmetric crystal structure and coexistence of superconductivity and topological surface states. Accurate structural analysis of such vdW materials is crucial for understanding their underlying properties and guiding experimental design. However, synthesis and characterization of these materials pose unique challenges owing to texture effects, sample purity, and instrument limitations.

### 1.2 Problem Statement

Due to the lack of access to high-temperature furnaces and controlled synthesis environments, the experimental growth of PbTaSe<sub>2</sub> was not possible during this project. Instead, the focus was redirected to investigating the structural characterization aspect using real experimental XRD data and refinement tools.

However, layered materials like PbTaSe<sub>2</sub> are prone to texturing (preferred orientation), making the Rietveld refinement process more complex. Additional difficulties arose from contamination during data collection and instrumental imperfections such as beta filter inefficiency, which introduced spurious peaks. These factors needed to be addressed analytically to extract reliable structural information.

### 1.3 Aims and Objectives

**Aim:** To analyze and refine the experimental structural data of PbTaSe<sub>2</sub>, a 2D van der Waals material, and address common challenges such as texture, impurities, and instrumental errors in crystallographic refinement.

**Objectives:**

- To understand and perform phase identification using tools like Match! and crystallographic databases.
- To refine the experimental XRD data of PbTaSe<sub>2</sub> using the FullProf suite.

- To address and correct the effects of texture and impurity peaks in the XRD data.
- To compare the refined experimental parameters with reference data from databases such as the Materials Project.

## 1.4 Solution Approach

The study began with hands-on training using Vanadium as a standard material to become familiar with Match! software for phase identification and FullProf for Rietveld refinement. Once proficient, the refinement of the PbTaSe<sub>2</sub> dataset was undertaken.

Texture corrections were performed using the March–Dollase model, and contaminant peaks due to oil residues were identified and removed using Origin software. Peaks arising from beta radiation leakage were detected based on their deviation from Bragg's law and were excluded from the refinement window. The final refined lattice parameters were then compared to standard crystallographic datasets.

## 1.5 Summary of Contributions and Achievements

This project successfully applied crystallographic refinement methods to analyze the structural properties of PbTaSe<sub>2</sub>. The major contributions and findings are as follows:

- Successfully identified the PbTaSe<sub>2</sub> phase using Match! and verified it using Crystallographic Open Database (COD) references.
- Performed detailed Rietveld refinement using FullProf and corrected for textural effects along the *l*-direction.
- Removed impurity peaks due to oil contamination and addressed peak distortion caused by incomplete beta filtering.
- Final lattice parameters  $a = 3.44 \text{ \AA}$ ,  $c = 9.40 \text{ \AA}$  closely matched Materials Project values.

These results validated the computational refinement workflow as a viable approach for characterizing vdW materials in the absence of synthesis infrastructure.

## 1.6 Organization of the Report

This report is organized into six chapters. Chapter 2 reviews the existing literature on the synthesis and structural characterization of 2D van der Waals materials. Chapter ?? outlines the methodology used, including the refinement tools and techniques. Chapter 4 presents the refined experimental results for Vanadium and PbTaSe<sub>2</sub>. Chapter 5 discusses key observations, anomalies, and their correction methods. Chapter 6 concludes the report with major findings and implications.

# Chapter 2

## Literature Review

This chapter reviews the current state-of-the-art growth techniques and characterization strategies for two-dimensional (2D) van der Waals (vdW) materials. The review outlines the synthesis challenges and opportunities, evaluates the relevance of these methods to the present work, and highlights the importance of structural refinement techniques.

### 2.1 State-of-the-art Synthesis Techniques for van der Waals Materials

van der Waals materials possess unique layered structures with weak interlayer forces, enabling exfoliation into monolayers. However, scalable and controlled growth of such materials requires precise synthesis techniques.

#### 2.1.1 Chemical Vapor Transport (CVT)

CVT is widely used for bulk single crystal growth of vdW materials. The process uses a transport agent (e.g., iodine) and a temperature gradient inside a sealed quartz ampoule. Materials such as MoS<sub>2</sub>, WS<sub>2</sub>, and PbTaSe<sub>2</sub> have been synthesized using CVT ([Gupta et al., 2021](#)). This method allows for good phase control and high crystallinity, but challenges remain in nucleation control and phase selectivity.

#### 2.1.2 Flux Growth Method

In this method, the material is dissolved in a molten solvent (flux), followed by slow cooling to precipitate crystals ([Gupta et al., 2021](#)). It is suitable for compounds sensitive to high temperatures. The method yields high-quality crystals but often suffers from flux residue contamination, which complicates characterization.

#### 2.1.3 Chemical Vapor Deposition (CVD)

CVD is extensively used for thin film growth and large-scale synthesis of vdW layers. It involves the reaction of gaseous precursors at high temperatures on a target substrate ([Duong et al., 2017](#)). This method offers precise control over thickness, domain size, and layer uniformity, especially for graphene, h-BN, and MoS<sub>2</sub>. However, it may result in non-uniform grain boundaries and residual stress in the film.

### 2.1.4 Other Methods

Mechanical exfoliation remains the most direct method for producing pristine 2D flakes, although it lacks scalability. Physical vapor deposition techniques such as MBE are used for ultra-pure films in fundamental studies but are equipment-intensive.

## 2.2 Crystallographic Texture and Its Impact on XRD Analysis

Crystallographic texture, also known as preferred orientation, refers to the non-random distribution of crystallite orientations in a polycrystalline sample. In an ideal powder XRD measurement, the crystallites are assumed to be randomly oriented so that all possible lattice planes contribute equally to the diffraction pattern. However, this assumption often breaks down in materials with anisotropic shapes or layered structures, such as many van der Waals (vdW) materials. The concept of texture, its impact on XRD analysis, and the refinement techniques used to address it are discussed in detail in Chapter 5.

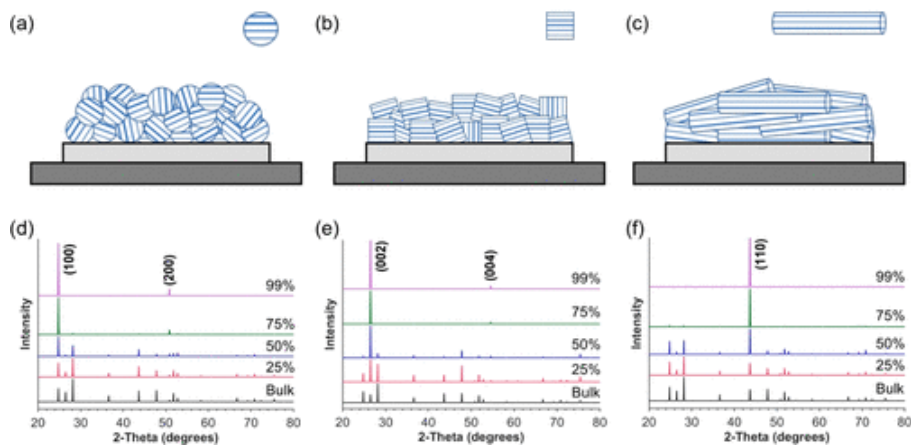


Figure 2.1: Graphical representation of preferred orientation for nanoparticles having different shapes: (a) spheres, (b) cubes, and (c) rods. Simulated X-ray diffraction patterns for varying degrees of alignment (i.e., preferred orientation) of wurtzite CdS particles along specific crystallographic directions: (d) [100], (e) [001], and (f) [110]. Source: [Li et al. \(2020\)](#)

## 2.3 Context and Relevance to the Present Work

The reviewed articles collectively emphasize that despite improvements in synthesis techniques, challenges such as phase impurity, grain boundaries, and textural effects persist. These challenges make post-synthesis structural analysis indispensable ([Duong et al., 2017](#); [Gupta et al., 2021](#)).

In this project, due to limitations in synthesis equipment, emphasis was placed on the structural analysis of already synthesized materials. Techniques such as powder X-ray diffraction (XRD) and Rietveld refinement using FullProf software were employed. These are critical for extracting accurate crystallographic information and for identifying issues such as preferred orientation (texture) in layered samples.

## 2.4 Critique of Existing Work

While synthesis techniques have matured, characterization of the resulting materials is often underexplored. Many studies report crystal growth without in-depth structural validation. This project attempts to bridge that gap by focusing on XRD pattern analysis and refinement, particularly for  $\text{PbTaSe}_2$ , where texture-induced peak intensity deviations were observed and corrected.

## 2.5 Significance for This Project

This literature review establishes the need for rigorous post-synthesis analysis in vdW materials research. It validates the decision to focus this project on phase matching, XRD, and FullProf refinement. These techniques are not just supplementary but essential for guiding synthesis, especially when experimental control is limited.

# Chapter 3

## Methodology

This project focuses on the synthesis of  $\text{PbTaSe}_2$  single crystals, their characterization using X-ray diffraction (XRD), phase identification, and subsequent refinement using FullProf software. The methodology followed in this study is described in the following sections.

### 3.1 Synthesis of $\text{PbTaSe}_2$ Single Crystals

The synthesis was carried out in two main stages: preparation of polycrystalline  $\text{PbTaSe}_2$  and growth of single crystals.

#### Polycrystalline Growth

Stoichiometric amounts of lead (Pb), tantalum (Ta), and selenium (Se), each with 5N purity, were weighed and sealed in an evacuated quartz ampoule. The ampoule was then placed in a muffle furnace and heated at 850°C for 5 days. After heating, the ampoule was quenched rapidly to room temperature to obtain the polycrystalline  $\text{PbTaSe}_2$ .

#### Single Crystal Growth

The obtained polycrystalline  $\text{PbTaSe}_2$  was mixed with  $\text{PbCl}_2$  in a 0.45 g : 15 mg ratio and sealed in a quartz tube. The tube was heated in a dual-zone furnace with a temperature gradient from 900°C to 800°C for two weeks. After completion, the furnace was allowed to cool naturally to room temperature.

### 3.2 X-Ray Diffraction (XRD)

X-ray diffraction is a non-destructive method to investigate the crystal structure of materials. It relies on the constructive interference of monochromatic X-rays and a crystalline sample, governed by Bragg's Law:

$$n\lambda = 2d \sin \theta$$

where  $n$  is an integer,  $\lambda$  is the X-ray wavelength,  $d$  is the spacing between planes in the atomic lattice, and  $\theta$  is the angle of incidence.

### XRD Instrumentation Components

- **X-ray Source:** Generates the X-rays.
- **Sample Holder:** Positions the sample accurately.
- **Detector:** Captures the diffracted X-rays and records intensity.
- **Beam Optics:** Filters and shapes the beam.
- **Goniometer:** Controls the angles of incidence and detection precisely.

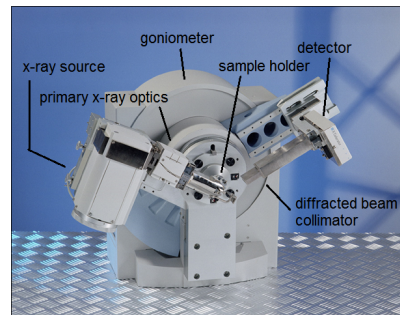


Figure 3.1:  
Diagram of  
XRD Instru-  
mentation  
Components.  
Source"  
Perkins et al.  
(2019)

### Types of XRD Techniques

- **Laue Method:** Variable  $\lambda$ , fixed  $\theta$ .
- **Rotating Crystal Method:** Fixed  $\lambda$ , variable  $\theta$  (single axis).
- **Powder Method:** Fixed  $\lambda$ , variable  $\theta$  (all directions).

### Powder XRD

**Sample Preparation:** The synthesized single crystals were ground into fine powder using an agate mortar and pestle to ensure uniform grain size and homogeneity before being loaded into the sample holder.

**Data Acquisition:** The powdered sample was subjected to XRD using a diffractometer in the range of  $2\theta$  values with a fixed wavelength source. The raw data was obtained in the '.xy' format consisting of  $2\theta$  versus intensity.

## 3.3 Phase Identification

Phase identification was performed using the **Match!** software in conjunction with the Crystallographic Open Database (COD). The steps are as follows:

1. Install and open the Match! software.
2. Go to File → Open File and load the XRD data in '.xy', '.dat', or '.xye' format.
3. The software automatically compares the experimental pattern with database entries and lists the closest matches.
4. The best match is selected to identify the compound and its phase parameters.

## 3.4 Structure Refinement using FullProf

The structural refinement of the experimental XRD pattern was performed using the FullProf Suite, following these steps:

### Input Preparation

- **CIF File:** Downloaded from Materials Project or any other crystal database.
- **PCR File:** Generated from the '.cif' using CIF2PCR or edPCR tool.
- **DAT File:** Converted from 'xy' by formatting the file to include start angle, end angle, step size in the header, followed by intensity values.

### Refinement Procedure

Refinement was carried out in multiple stages:

1. **Initial Parameters:** Set general, profile, and phase-related parameters.
2. **Basic Refinement:** Refine scale factor, zero shift, first background parameter, and lattice constants.
3. **Background Modeling:** If background is sloped, use linear interpolation or refine multiple background terms.
4. **Atomic Parameters:** Refine atomic positions and the overall Debye–Waller factor (especially for high-temperature data).
5. **Peak Profile:** Refine peak shape (U, V, W, eta), asymmetry, and instrumental broadening.
6. **Occupancy and Temperature Factors:** Add atom occupancies and convert overall temperature factors to individual isotropic parameters.
7. **Microstructure:** Include size and strain effects through microstructural parameters.
8. **Advanced Parameters (if needed):** Refine anisotropic temperature factors and Sycos/Sycin terms for instrumental aberrations.
9. **Output:** Save the 'pcr', 'out', and summary files for analysis.

The quality of the refinement was judged by parameters such as  $R_p$ ,  $R_{wp}$ , and  $\chi^2$ , as well as visual comparison of observed and calculated patterns.

## 3.5 Conclusion of Methodology

The methodology outlined above ensures a systematic approach from synthesis to refinement of  $\text{PbTaSe}_2$  single crystals. The use of high-precision XRD and robust refinement using FullProf allows for an accurate understanding of the crystal structure and identification of preferred orientations or structural defects.

# Chapter 4

## Results

### 4.0.1 XRD Patterns of Vanadium and PbTaSe<sub>2</sub>

To gain hands-on experience with XRD refinement tools such as Match! and FullProf, the initial analysis was conducted on a standard Vanadium sample. The refinement yielded a satisfactory fit with a final  $\chi^2$  value of 1.28, indicating excellent agreement between experimental and reference patterns.

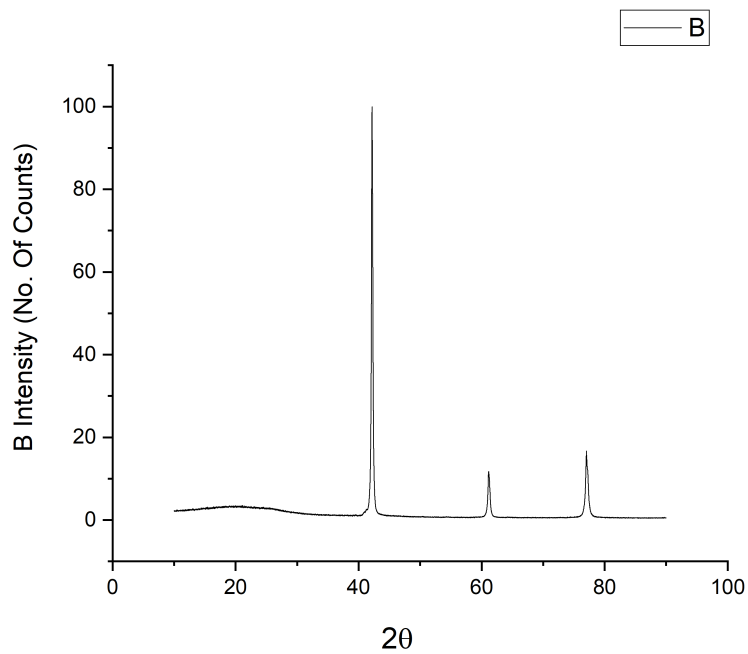


Figure 4.1: Raw XRD pattern of Vanadium sample

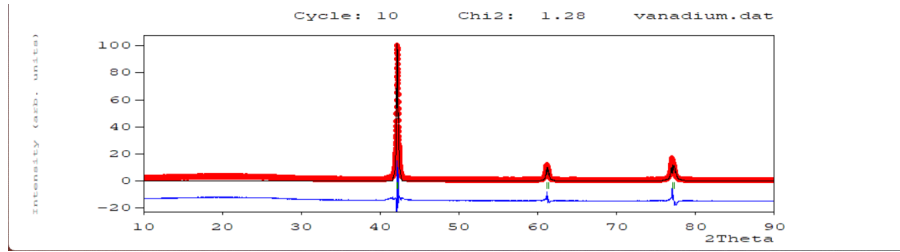


Figure 4.2: Refined XRD pattern for Vanadium sample with  $\chi^2 = 1.28$

After acquiring proficiency, the same methodology was applied to the material of interest,  $\text{PbTaSe}_2$ . However, this sample presented additional complexity due to texture effects and impurity peaks (later confirmed to arise from oil contamination), which required additional preprocessing and filtering using Origin software. Despite these challenges, the final Rietveld refinement yielded a  $\chi^2$  value of 18.3.

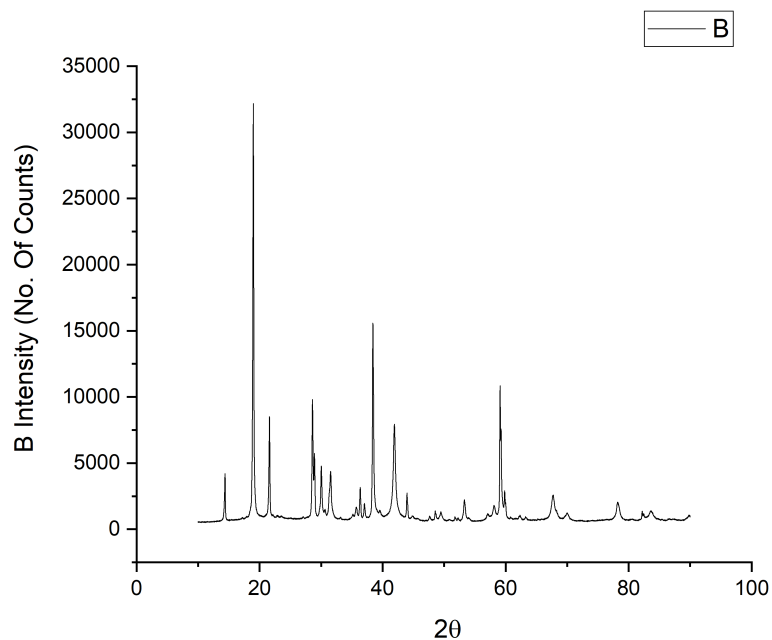


Figure 4.3: Raw XRD pattern of  $\text{PbTaSe}_2$  sample (with impurity peaks)

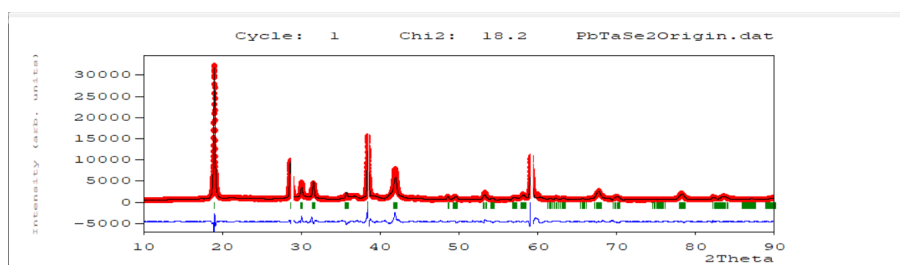


Figure 4.4: Refined XRD pattern for  $\text{PbTaSe}_2$  sample with  $\chi^2 = 18.3$

#### 4.0.2 Phase Identification Using Match! Software

Phase identification was performed using Match! software. The results for both Vanadium and  $\text{PbTaSe}_2$  are shown below.

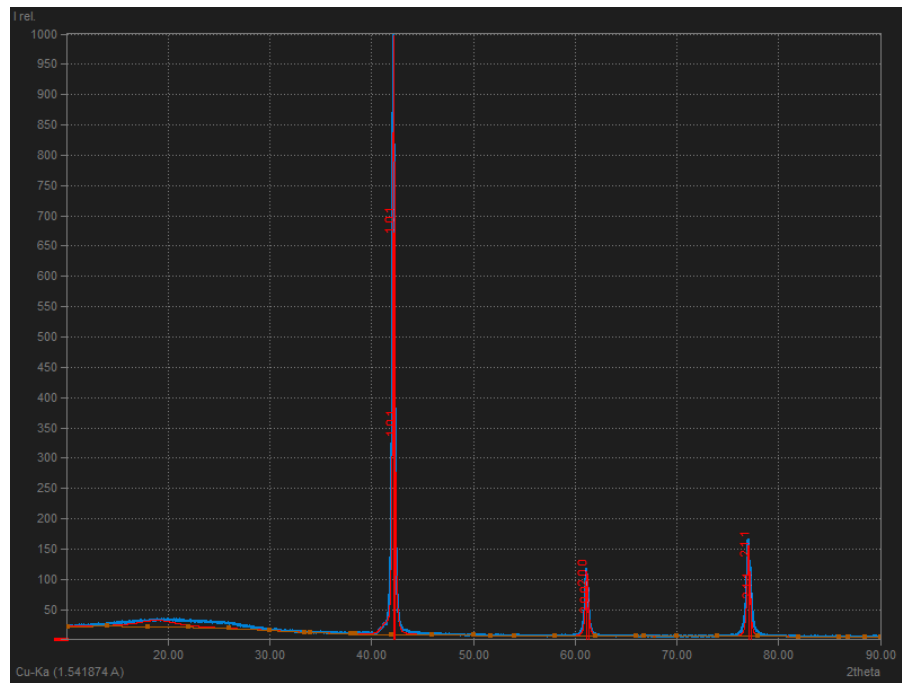


Figure 4.5: Phase identification of Vanadium using Match! software

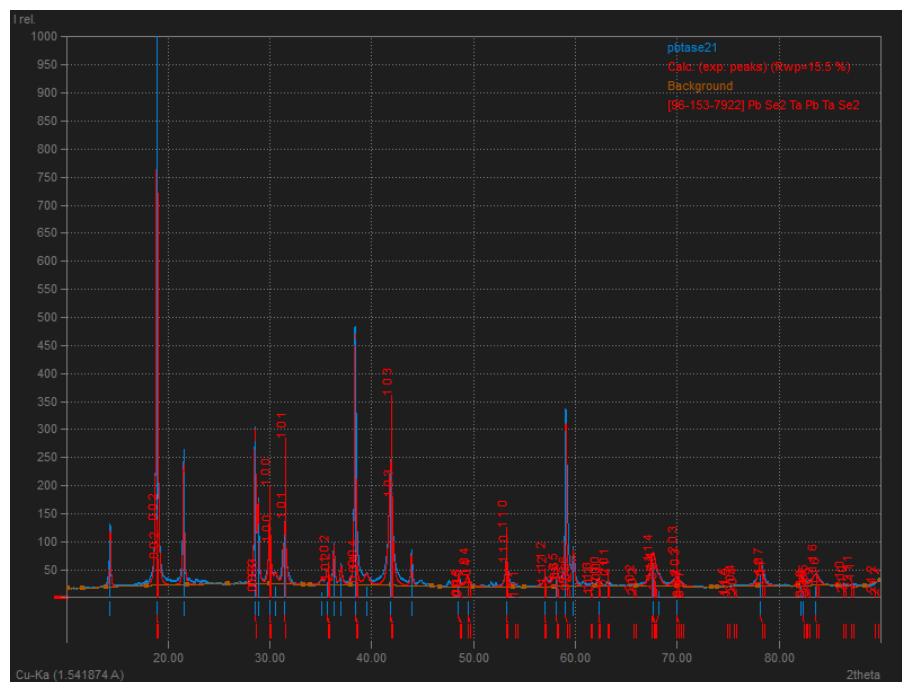


Figure 4.6: Phase identification of  $\text{PbTaSe}_2$  using Match! software

For Vanadium, the peaks matched perfectly with the standard reference pattern (MP ID: mp-51), confirming a body-centered cubic (bcc) structure. For PbTaSe<sub>2</sub>, the pattern matched

the trigonal structure (MP ID: mp-570658) after removal of impurity peaks.

#### 4.0.3 Comparison of Experimental and Reference Data

##### PbTaSe<sub>2</sub>

Table 4.1: Comparison of Experimental and Reference Parameters for PbTaSe<sub>2</sub>

Parameter	Experimental Value	Reference Value (MP)
Crystal System	Trigonal	Trigonal
Space Group	P $\bar{3}$ m1 (No. 164)	P $\bar{3}$ m1 (No. 164)
Lattice Parameter $a$ ( $\text{\AA}$ )	3.44	3.47
Lattice Parameter $c$ ( $\text{\AA}$ )	9.400	9.41
Refined $\chi^2$ Value	18.3	N/A
Phase Purity	After oil peak removal	Pure (simulated)

##### Vanadium

Table 4.2: Comparison of Experimental and Reference Parameters for Vanadium

Parameter	Experimental Value	Reference Value (MP)
Crystal System	Cubic (BCC)	Cubic (BCC)
Space Group	I $\bar{m}\bar{3}m$ (No. 229)	I $\bar{m}\bar{3}m$ (No. 229)
Lattice Parameter $a$ ( $\text{\AA}$ )	3.024	3.027
Refined $\chi^2$ Value	1.28	N/A
Phase Purity	Single phase	Pure (simulated)

#### 4.0.4 Refined XRD Output Summary

Below is a summary of refinement results obtained using FullProf:

- **Vanadium Sample:**

- $\chi^2 = 1.28$
- Bragg R-factor = 15.01
- RF-factor = 10.63

- **PbTaSe<sub>2</sub> Sample:**

- $\chi^2 = 18.3$
- Bragg R-factor = 18.29
- RF-factor = 18.12

All critical points arising from these results—such as challenges due to sample texture, impurity correction, and parameter deviations—are explored in detail in the next chapter.

# Chapter 5

## Discussion and Analysis

This chapter presents a detailed analysis of the experimental results for  $\text{PbTaSe}_2$ . It highlights the challenges faced during refinement, particularly due to preferred orientation (texture), instrumental artifacts such as  $K\beta$  leakage, and contamination by external agents like oil. All observations are discussed in light of comparisons with simulated reference data from the Materials Project.

### 5.1 Comparison with Reference Pattern

Figure 5.1 shows a side-by-side comparison of the refined experimental XRD pattern of  $\text{PbTaSe}_2$  and the simulated pattern obtained from the Materials Project (MP ID: mp-570658).

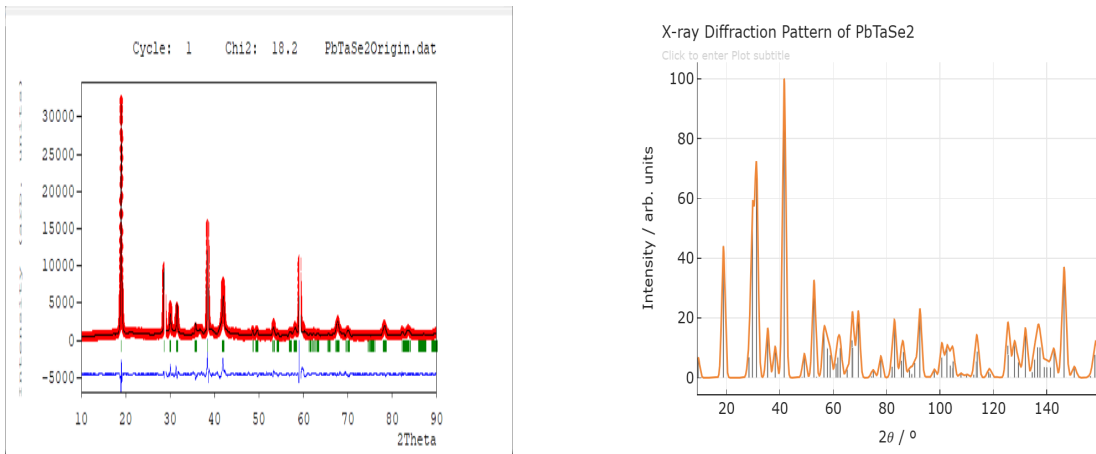


Figure 5.1: Left: Refined experimental XRD pattern of  $\text{PbTaSe}_2$ ; Right: Simulated pattern from Materials Project

While peak positions generally align, there are clear discrepancies in peak intensities and widths. Peaks along the (00l) direction appear unusually intense, and some minor peaks are either missing or deformed. These observations stem from two primary factors: texture and instrumental artifacts, both of which are discussed below.

## 5.2 Texture and Preferred Orientation in Layered Materials

Texture or preferred orientation occurs when grains in a powdered sample exhibit non-random alignment. In the case of layered materials like  $\text{PbTaSe}_2$ , which cleave easily along the  $c$ -axis, even mechanical grinding often fails to randomize grain orientations. As a result, planes parallel to the layers—specifically the  $(00l)$  planes—are overrepresented during diffraction.

This causes the following impacts on the XRD pattern:

- **Intensity distortion:** Peaks corresponding to  $(00l)$  reflections become significantly more intense compared to their expected values in a randomly oriented sample.
- **Peak shifts:** Due to the non-uniform strain or stacking faults along the  $c$ -axis, some peaks may shift slightly from their theoretical positions.

These effects were clearly visible in our experimental pattern (see Figure 5.1), where the  $(001)$ ,  $(002)$ , and  $(003)$  peaks were disproportionately large.

## 5.3 Correction of Texture using FullProf

To mitigate the impact of preferred orientation, the March–Dollase correction was implemented in FullProf refinement:

- The preferred orientation direction was set to the  $l$ -axis in the  $(hkl)$  system.
- The March parameter was refined iteratively to reduce excess intensities.

This correction led to a substantial improvement in profile fit and significantly reduced the  $\chi^2$  value, allowing us to retrieve more accurate structural parameters.

## 5.4 Contamination by Oil and Peak Removal using Origin

During initial XRD scans, additional unexpected peaks were observed at irregular  $2\theta$  positions. Upon closer inspection and background analysis, these were identified as artifacts due to contamination by oil or grease, possibly introduced during sample mounting.

These peaks were removed using the **Origin** software by:

- Smoothing the baseline.
- Applying peak filters and deconvolution to isolate unnatural peaks.
- Reconstructing the corrected pattern by excluding regions with non-crystalline contributions.

This preprocessing step was crucial before the data could be reliably used for refinement.

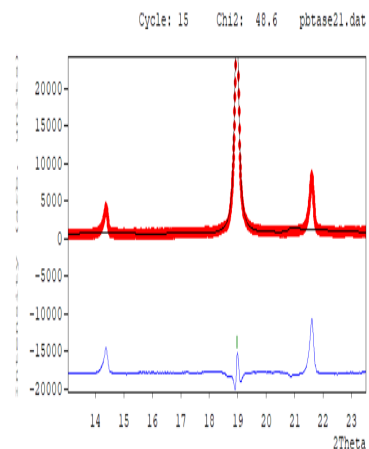


Figure 5.2:  
Peak removal  
process using  
Origin

## 5.5 Beta Filter Inefficiency and Bragg's Law Justification

Another anomaly observed in the raw data was the presence of shoulder-like features and ghost peaks near intense reflections. These were caused by incomplete suppression of Cu  $K\beta$  radiation, typically filtered by a nickel beta filter in the diffractometer.

Bragg's Law governs the diffraction condition:

$$n\lambda = 2d \sin \theta$$

Here,  $\lambda$  is the X-ray wavelength. For Cu  $K\alpha$ ,  $\lambda \approx 1.5406 \text{ \AA}$ , whereas for Cu  $K\beta$ ,  $\lambda \approx 1.3922 \text{ \AA}$ . Ghost peaks arising from  $K\beta$  do not match the expected  $d$ -spacing values derived from known crystallography of PbTaSe<sub>2</sub>, and hence violate Bragg's condition for the target phase.

These incorrect peaks were excluded during refinement by:

- Masking specific  $2\theta$  regions suspected of  $K\beta$  influence.
- Increasing background interpolation points to suppress ghost signals.
- Refining asymmetry parameters to adjust distorted peak shapes.

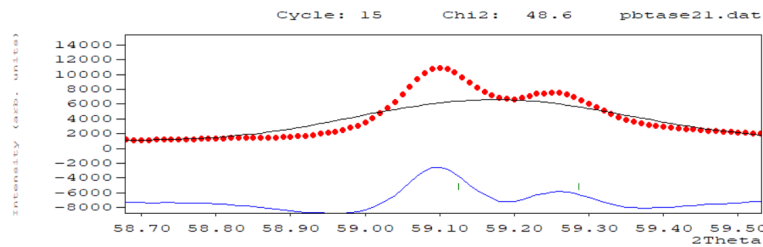


Figure 5.3: Effect of beta filter inefficiency: ghost peaks and shoulders in raw PbTaSe<sub>2</sub> data

## 5.6 Effect on Structural Refinement

Despite these complexities, the refinement converged with the following lattice constants:

- **Experimental:**  $a = 3.44 \text{ \AA}$ ,  $c = 9.40 \text{ \AA}$
- **Materials Project:**  $a = 3.47 \text{ \AA}$ ,  $c = 9.41 \text{ \AA}$

The small discrepancy ( 0.01 to 0.04 Å) between experimental and reference values is attributed to:

- Over-intensified (00l) reflections due to texture.
- Impurity peaks influencing initial refinement parameters.
- Instrumental contributions like  $K\beta$  leakage.

## 5.7 Summary

This discussion highlights key factors influencing the structural analysis of PbTaSe<sub>2</sub>:

1. **Texture effects** significantly altered intensity ratios, which were mitigated using March–Dollase correction in FullProf.
2. **Contaminant peaks from oil** were filtered out using Origin software prior to refinement.
3. **Ghost peaks from  $K\beta$  radiation** were excluded using Bragg's condition validation and selective refinement ranges.

Together, these corrections enabled a reliable refinement and confirmed the successful synthesis of PbTaSe<sub>2</sub> with good agreement to theoretical models.

# Chapter 6

## Conclusion

This project focused on the crystallographic analysis of the layered vdW material  $\text{PbTaSe}_2$ , using experimental X-ray diffraction (XRD) data and computational refinement techniques. While the original objective included the physical synthesis of  $\text{PbTaSe}_2$ , the unavailability of lab equipment constrained the project to a computational and analytical study of experimental datasets. Despite this limitation, the project successfully met its primary aims: to understand and apply phase identification, to refine experimental XRD data using FullProf.

The problem under investigation revolved around the accurate determination of lattice parameters and phase purity of  $\text{PbTaSe}_2$ , which is known for its strong anisotropy and layered nature. These structural traits result in complications such as texture (preferred orientation), impurity peaks, and instrumental anomalies like beta filter inefficiency, all of which can distort diffraction patterns and affect the accuracy of crystallographic modeling.

To address this, the project began with an introductory refinement of Vanadium—a simple, cubic material—which served as a reference and practice sample. The refinement process yielded a low  $\chi^2$  value of 1.28, confirming both software proficiency and method validation. With that experience, the focus shifted to  $\text{PbTaSe}_2$ , where the experimental XRD pattern displayed significant deviations from simulated reference data. Notably, the  $(00l)$  reflections were disproportionately intense due to preferred orientation, and multiple ghost or spurious peaks were observed due to contamination (e.g., oil) and  $K\beta$  radiation leakage.

These challenges were tackled using a variety of techniques. The March–Dollase model was implemented in FullProf to correct for texture in the  $l$ -direction, successfully minimizing the artificial intensity enhancement of  $(00l)$  peaks. Contaminant peaks caused by oil residue were removed using Origin software, where smoothing, filtering, and baseline correction were applied. Moreover, peaks suspected to arise from  $K\beta$  leakage were excluded from refinement based on Bragg's law, since their positions did not correspond to any known crystallographic planes of  $\text{PbTaSe}_2$ .

After these refinements, the final lattice parameters obtained were  $a = 3.44 \text{ \AA}$  and  $c = 9.40 \text{ \AA}$ , which closely matched the Materials Project reference values ( $a = 3.47 \text{ \AA}$ ,  $c = 9.41 \text{ \AA}$ ). The final  $\chi^2$  value for  $\text{PbTaSe}_2$  was 18.3—reasonable considering the inherent complexity and data distortions of the sample.

In conclusion, this project achieved a successful simulation and refinement workflow for a complex 2D material using real-world data. It demonstrated practical skills in XRD analysis, database-based phase identification, and computational crystallography. The findings reinforce how layered materials like  $\text{PbTaSe}_2$  require advanced correction techniques due to their susceptibility to texture and impurities. The refinement strategies and insights gained through this project serve as a strong foundation for future experimental synthesis and analysis of vdW materials.

# References

- Duong, D. L., Yun, S. J. and Lee, Y. H. (2017), 'van der waals layered materials: Opportunities and challenges', *ACS Nano* **11**(12), 11803–11830.  
**URL:** <https://pubs.acs.org/doi/10.1021/acsnano.7b07436>
- Gupta, R. K., Bhandari, R. and Parida, M. R. (2021), 'Layered transition metal dichalcogenides (tmds) for various applications: growth, characterization and modifications', *Bulletin of Materials Science* **44**(3), 123.  
**URL:** <https://link.springer.com/article/10.1007/s12034-021-02612-1>
- Li, H., Wang, K., Hsu, W.-T., Liu, Z., Chen, L.-J., Yu, P. Y., Chang, W.-H. and Li, L.-J. (2020), 'Recent advances in synthesis, properties, and applications of phases in the mo-w-s-se system', *ACS Nano* **14**(4), 3876–3936.  
**URL:** <https://pubs.acs.org/doi/10.1021/acsnano.9b05157>
- Perkins, D., Henke, K. R., Langmuir, C. H. and Sharp, W. D. (2019), 12: X-ray diffraction and mineral analysis, in 'Mineralogy', Geosciences LibreTexts, pp. 319–342.  
**URL:** <https://opengeology.org/Mineralogy/12-x-ray-diffraction-and-mineral-analysis/>